

Aspect Ratio Dependence of the Elastic Properties of ZnO Nanobelts

Marcel Lucas,^{*,†} Wenjie Mai,[‡] Rusen Yang,[‡] Zhong Lin Wang,^{*,‡} and Elisa Riedo^{*,†}

School of Physics, Georgia Institute of Technology, Atlanta, Georgia 30332-0430, and School of Materials Science and Engineering, Georgia Institute of Technology, Atlanta, Georgia 30332-0245

Received February 7, 2007

ABSTRACT

The Young's modulus of ZnO nanobelts was measured with an atomic force microscope by means of the modulated nanoindentation method. The elastic modulus was found to depend strongly on the width-to-thickness ratio of the nanobelt, decreasing from about 100 to 10 GPa, as the width-to-thickness ratio increases from 1.2 to 10.3. This surprising behavior is explained by a growth-direction-dependent aspect ratio and the presence of stacking faults in nanobelts growing along particular directions.

Zinc oxide (ZnO) has drawn considerable interest because of its semiconducting and piezoelectric properties.^{1,2} A rich variety of ZnO nanostructures, such as nanocombs, nanorings, nanosprings, nanobelts, nanowires, and nanocages, can be synthesized.³ ZnO nanostructures have applications as field-effect transistors,⁴ gas sensors,⁵ field-emission displays,⁶ and nanoelectromechanical systems (NEMS).⁷ All of these applications require the knowledge and the ability to control the mechanical behavior of ZnO nanostructures. In particular, it is of crucial importance to understand the size dependence of the elastic properties.

In general, size-dependent effects can be found when the volume of a nanostructure is so small that surface effects start to be relevant. This usually happens for dimensions smaller than tens of nanometers, while for larger sizes, the Young's modulus approaches its bulk value.^{8–10} For example, the Young's modulus of carbon nanotubes increases significantly with decreasing size for diameters smaller than 4 nm.⁸ Conversely, the modulus of GaN nanowires increases with increasing diameter, reaching the bulk value at 84 nm.⁹ The origin of the elastic modulus size dependence has been related to different effects such as the presence of defects^{9,11} and the balance between surface and bulk properties as the surface-to-volume ratio varies.^{10,12}

The elastic properties of ZnO nanostructures and their size dependence have been previously investigated by means of transmission electron microscopy (TEM)^{10,13,14} and atomic force microscopy (AFM).^{15,16} The Young's modulus of ZnO nanowires was found to decrease dramatically with increasing diameter, reaching the ZnO bulk value for diameters larger

than 120 nm. This behavior was attributed to a surface stiffening effect dominating at large surface-to-volume ratios.¹⁰ The Young's modulus of ZnO nanobelts with a wide range of lateral dimensions, ranging from 20 to 230 nm in thickness and 30 to 700 nm in width, was also measured. Previous studies yielded a wide spread of modulus values between 30 and 160 GPa, without a clear dependence on their thickness t , width w , or surface-to-volume ratio.^{13–16} Molecular dynamics simulations showed a noticeable size dependence of the elastic properties only for ZnO nanobelts with lateral dimensions below 4 nm, for which the effects of surface stresses become significant.¹⁷

In this letter, the elastic properties of ZnO nanobelts are investigated with an AFM by means of the modulated nanoindentation technique. Their Young's modulus is found to decrease significantly from about 100 to 10 GPa, as the width-to-thickness ratio increases from 1.2 to 10.3. This behavior is explained by a growth-direction-dependent aspect ratio and the presence of stacking faults in nanobelts growing along particular directions.

In the modulated nanoindentation technique,⁸ a modulated signal induces a normal oscillation of the scanner supporting the sample, while the normal force is monitored by the deflection of the cantilever (Figure 1a). The frequency of the oscillations was set at 1.384 kHz, and the amplitude was maintained low at 1.5 Å to remain in the sticking regime. The normal force F necessary to move vertically the substrate of the nanobelt by d_{tot} with respect to the cantilever support is equivalent to the force needed to elastically stretch two springs in series: the cantilever, with normal stiffness k_{lever} , and the tip-sample contact with normal stiffness k_{contact} . k_{contact} is measured at different normal forces using:

$$\partial F / \partial d_{\text{tot}} = (1/k_{\text{lever}} + 1/k_{\text{contact}})^{-1} \quad (1)$$

* Corresponding authors. E-mail: marcel.lucas@gatech.edu (M.L.); zhong.wang@mse.gatech.edu (Z.L.W.); elisa.riedo@physics.gatech.edu (E.R.).

[†] School of Physics, Georgia Institute of Technology.

[‡] School of Materials Science and Engineering, Georgia Institute of Technology.

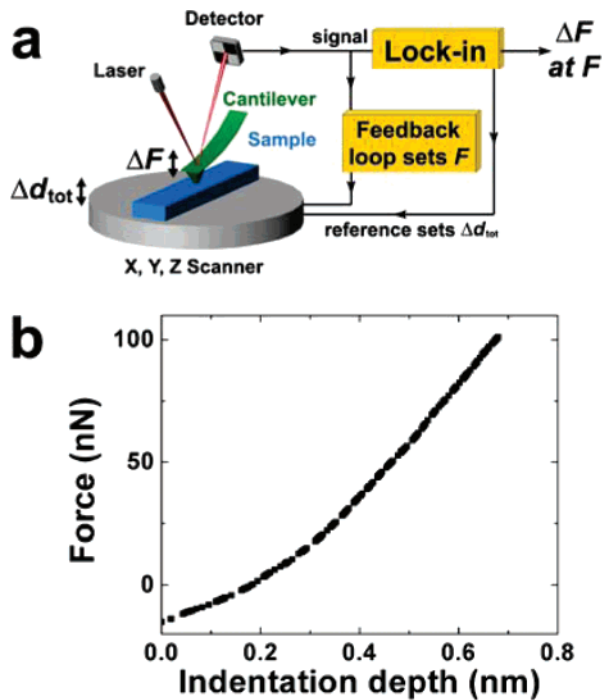


Figure 1. (a) Experimental setup for the modulated nanoindentation method. (b) Normal force as a function of indentation depth for a nanobelt of width-to-thickness ratio 2.9.

Because the width of the nanobelt is much larger than the tip radius, the tip-sample contact can be modeled as a sphere indenting a flat surface, in which case, the Young's modulus can be extracted from:

$$k_{\text{contact}} = 2E^*a \quad (2)$$

with a the contact radius and $E^* = [(1 - \nu_1^2)/E_1 + (1 - \nu_2^2)/E_2]^{-1}$, where ν_i and E_i are the Poisson's ratio and Young's modulus of the indenter ($i = 1$) and sample ($i = 2$), respectively. The following values were used in this study: $\nu_1 = 0.27$, $E_1 = 169$ GPa for the silicon tip, and $\nu_2 = 0.3$, an average value calculated using the elastic constants tabulated in ref 18. The contact radius a is given by the Hertz model:

$$a^3 = \frac{3}{4} \frac{R \cdot (F + F_{\text{adh}})}{E^*} \quad (3)$$

where R is the tip radius and F_{adh} is the tip-sample adhesion force which is experimentally determined.^{8,19} The indentation depth z is obtained by integrating k_{contact} obtained at different values F' of the normal force:

$$z(F) = \int_{F(z=0)}^{F_{\text{max}}} \frac{dF'}{k_{\text{contact}}(F')} \quad (4)$$

where F_{max} is the maximum normal force used in the experiments. $F(z = 0)$ can be negative due to the presence of adhesive forces (Figure 1b). This modulated nanoindentation technique has been tested on a silicon substrate,

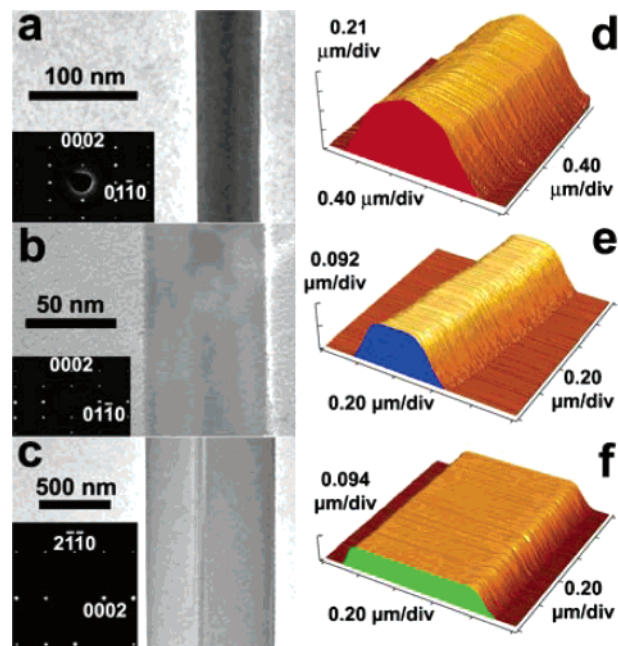


Figure 2. TEM images of (a) nanowire; (b) nanobelt grown along the [0001] direction; (c) nanobelt grown along the [2110] direction with a stacking fault parallel to the (0001) surface and present over the entire length of the nanobelt. Insets show the corresponding electron diffraction pattern. We note that the nanobelt in (c) is wider than 500 nm, thus by comparison with the AFM measurements in Figure 3, we conclude that in this nanobelt the narrow side surface is the (0001). AFM images of (d) nanowire ($2 \mu\text{m} \times 2 \mu\text{m}$ image); (e) nanobelt with a width-to-thickness ratio of 1.9 ($1 \mu\text{m} \times 1 \mu\text{m}$ image); (f) nanobelt with a width-to-thickness ratio of 9.5 ($1 \mu\text{m} \times 1 \mu\text{m}$ image).

yielding an average value of 143 GPa. The same silicon tip (PointProbe NCHR from Nanoworld), of radius around 60 nm, was used for the images and the modulated nanoindentation experiments. The normal cantilever spring constant, 33 N/m, was calibrated using the method of Sader et al.²⁰

The ZnO nanobelts were prepared by physical vapor deposition, following the procedure described by Pan et al.,²¹ and deposited on a flat silicon substrate. The nanobelts were characterized by TEM and AFM (Veeco CP-II). TEM images and electron diffraction patterns show that the ZnO nanobelts have a wurtzite structure and grow mainly along [0001] without defects or dislocations (Figure 2a,b). There are indications that a few of these nanobelts are actually nanowires, i.e., no rectangular or square cross section (Figure 2a). Less common growth directions are [0110] and [2110]. Nanobelts grown along these directions present the polar (0001) surface at the side surfaces. Figure 2c shows a TEM image of a nanobelt grown along the [2110] direction with the polar (0001) surface on the narrower side. This nanobelt presents a single stacking fault running parallel to the (0001) surface over the entire length of the nanobelt (Figure 2c), consistent with previous observations of stacking faults parallel to the (0001) surface.²¹

The distribution of the nanobelts growth direction is somehow reflected in the size and shape distribution of the nanobelts as observed by AFM (see Figures 2d-f and 3a-c). A statistical study of 137 nanobelts shows that 85%

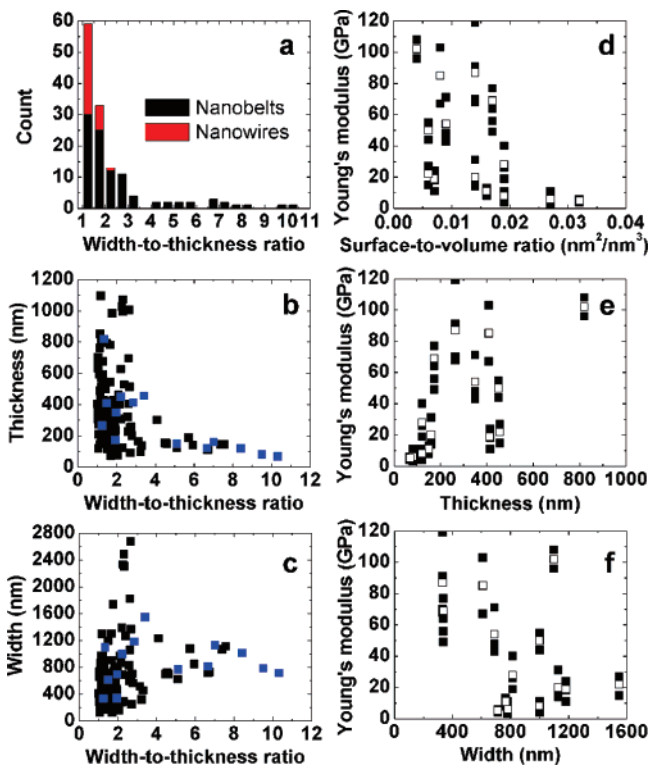


Figure 3. Characteristics of 137 ZnO nanostructures determined by AFM: (a) width-to-thickness ratio distribution, (b) thickness against width-to-thickness ratio, and (c) width against width-to-thickness ratio. The Young's modulus of 14 (blue symbols) of the nanobelts analyzed in (a), (b), and (c) is plotted as a function of (d) surface-to-volume ratio, (e) thickness, and (f) width. In (d–f), the solid symbols are data points, and the open symbols are average values of the measurements from the same nanobelt.

of them have a width-to-thickness ratio, w/t , smaller than 3 (Figures 3a, 2d,e). Among these nanobelts, 27% present a circular/polygonal cross section, characteristic of nanowires. For these nanowires, the average w/t is $w/t = 1.4 \pm 0.2$ (see Figures 3a and 2d). Finally, only 15% of the nanobelts have $3 < w/t < 10$ (see Figures 3a and 2f).

To investigate the size dependence of the elastic properties of ZnO nanobelts, the Young's modulus, E_{NB} , of 14 different nanostructures (nanobelts or nanowires) was measured as a function of surface-to-volume ratio, w , and t (see Figures 3d,f). No clear correlation has been found between E_{NB} and surface-to-volume ratio, w , and t . The surface-to-volume ratio is defined here as the ratio between the perimeter and the area of the cross section. Because most of the nanobelts are more than 100 μm long (the smallest length being 40 μm), the error due to end effects is less than 1%. Among the nanobelts studied here, a few have similar w or t but different w/t . For example, two nanobelts with comparable thicknesses, $t = 174$ nm and $t = 161$ nm but different w/t of 1.94 and 7.01 have average moduli of 69 and 20 GPa, respectively. Similarly, two nanobelts with $w \sim 1000$ nm but $w/t = 2.22$ and 8.21, have average moduli of 50 and 8 GPa, respectively. These results suggest that the key parameter controlling the elastic properties of the nanobelts is the width-to-thickness ratio.

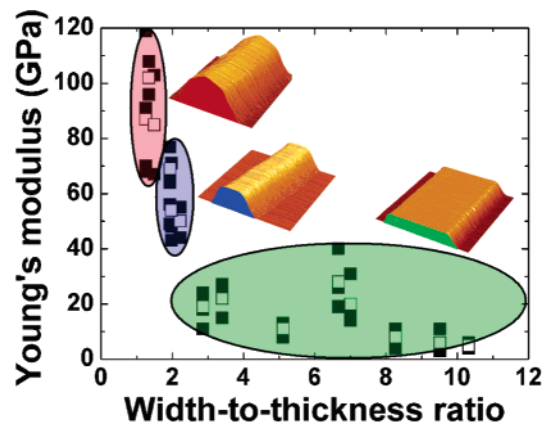


Figure 4. Young's modulus of ZnO nanostructures as a function of width-to-thickness ratio. The solid symbols are the data points, the open ones are the average value of the measurements from the same nanostructure. The red area corresponds to nanowires, the blue area to nanobelts with a low width-to-thickness ratio, and the green area to nanobelts with a high width-to-thickness ratio. The nanobelt cross section is highlighted with matching colors (inset).

Figure 4 shows E_{NB} against w/t for ZnO nanobelts. A clear tendency emerges from this graph, showing that the Young's modulus decreases from about 100 GPa to about 10 GPa as w/t increases from 1.2 to 10.3. A sharp decrease is observed for ratios between 2 and 3, while for ratios over 3, the Young's modulus remains constant. The w/t dependence of the Young's modulus presented in Figure 4 is highlighted in this paper for the first time. It is noted that data previously reported in the literature agree with the results shown here (see Supporting Information). The results compiled from refs 13 to 16 indicate that the highest Young's moduli, above 100 GPa, were measured for nanobelts with the smallest w/t , usually lower than 1.5. Yum et al. measured the elastic modulus of four ZnO nanobelts with $1.4 < w/t < 4.4$ and obtained $85 > E_{NB} > 38$ GPa, with $E_{NB} = 85$ GPa corresponding to $w/t = 1.4$.¹⁴ The results presented here are also consistent with the conclusions of ref 15, in which the elastic modulus is almost constant and equal to about 30 GPa for nanobelts with w/t ranging from 2 to 9.

To understand the origin of the low elastic modulus of nanobelts with high w/t , surface effects and the possibility of a structural phase transition were investigated. Chen et al. explained the size dependence of ZnO nanowires moduli by considering the nanowire as a composite wire composed of a core with a modulus similar to the bulk and a shell with a higher modulus.¹⁰ The observed increase of the modulus with a decreasing diameter of the wires is thus explained in terms of composite modulus, where the higher shell modulus dominates at large surface-to-volume ratios. However, the surface-to-volume ratio reported in our study is more than 1 order of magnitude smaller than the value required for noticeable surface effects in their investigation (0.004–0.032 compared with 0.08 nm^{-1}).

A structural phase transition can lead to a sudden stress drop and therefore an apparently low Young's modulus in the nanobelts. At a pressure around 9 GPa, a phase transition was observed in ZnO crystals²² and theoretical studies suggested that the phase transition pressure could be as low

as 6 GPa.^{23–25} Considering a maximum load F of 200 nN used in our experiments, $E^* = 75$ GPa, a tip radius of 60 nm, eq 3 would give a contact radius of 5 nm, and thus a maximum pressure of only 3 GPa. Indeed, no hysteresis or sudden force variations have been observed in our experiments when the tip is approaching or retracting during the indentation process. A power-law fit of the force-indentation depth curve yields an exponent of 1.50 ± 0.05 , in excellent agreement with the value $^{3/2}$, predicted by the Hertz contact mechanics model (Figure 1b).

Because no surface effects or structural phase transitions can be invoked to explain the observed w/t dependence, it is necessary to understand if w/t is related to any structural property of the nanobelts. Recent X-ray diffraction results on single ZnO nanobelts suggest a relationship between w/t and the growth direction. Nanobelts with $w/t = 8.5$ and 8.7 grew along $[01\bar{1}0]$, i.e., perpendicular to $[0001]$ and with a polar narrow side surface, while nanobelts with $w/t = 1.5$ and 2.1 grew along $[0001]$.²⁶ These findings are also consistent with the TEM and AFM measurements shown in Figures 2 and 3 and suggest that high w/t is less common and is associated to a less common growth direction, i.e., $[2\bar{1}\bar{1}0]$ or $[01\bar{1}0]$.

However, in bulk ZnO, the Young's modulus along $[0001]$ is expected to be close to the one along a perpendicular direction, i.e., $[2\bar{1}\bar{1}0]$ or $[01\bar{1}0]$.²⁷ By means of a commercial indentation system with a $1.5 \mu\text{m}$ diamond tip, the Young's moduli along the $[0001]$ and $[01\bar{1}0]$ directions were measured to be 163 and 143 GPa, respectively.²⁸ This result was confirmed by applying the modulated nanoindentation technique presented here to two ZnO bulk samples (MTI Corporation). The measured moduli are $E = 180$ GPa for the sample oriented (0001) and $E = 153$ GPa for the sample oriented $(01\bar{1}0)$.

Figure 2 and previous TEM measurements²¹ indicate that nanobelts or nanowires grown along $[0001]$ are free of dislocations and stacking faults, while nanobelts grown along $[01\bar{1}0]$ and $[2\bar{1}\bar{1}0]$ with the polar (0001) surface as the narrower side surface exhibit stacking faults parallel to the (0001) surface over the entire length of the nanobelts. We conclude that the low Young's modulus in nanobelts with high w/t is due to the presence of planar defects in nanobelts grown along $[01\bar{1}0]$ or $[2\bar{1}\bar{1}0]$ and identified as high w/t nanobelts. A similar role of the planar defects has been recently shown in WO_3 nanowires, where the Young's modulus decreases from about 300 GPa (bulk value) to 100 GPa, as the diameter of the nanowire increases from 16 to 53 nm. The cause of this behavior was attributed to a size-dependent defect concentration.¹¹

The origin of a larger Young's modulus for nanobelts with $w/t = 1$ as compared with nanobelts with $w/t = 2$ is still unclear. However, we remark that the majority of the nanobelts presenting the highest modulus values were identified as nanowires from AFM topography measurements. The symmetry of the structure seems thus to play a role.

In summary, the Young's modulus of ZnO nanobelts with a width-to-thickness ratio between 1.2 and 10.3 was measured by AFM using the modulated nanoindentation tech-

nique. We show that the modulus decreases with increasing width-to-thickness ratio from about 100 GPa to about 10 GPa. This unusual aspect ratio dependence is explained in terms of a growth-direction-dependent aspect ratio and the presence of stacking faults in nanobelts growing along particular directions. Our findings open the way to tailor the mechanical properties of the nanobelts in a controlled manner over a wide range of elastic modulus values.

Acknowledgment. We acknowledge the financial support from the DoE under grant no. DE-FG02-06ER46293, NSF. We thank Professor K. Gall and Professor Min Zhou for useful discussions and for providing the bulk ZnO samples.

Supporting Information Available: Review of data available on the mechanical properties of ZnO nanobelts. This material is available free of charge via the Internet at <http://pubs.acs.org>.

References

- (1) Wang, Z. L.; Song, J. H. *Science* **2006**, *312*, 242–246.
- (2) Zhao, M.-H.; Wang, Z. L.; Mao, S. X. *Nano Lett.* **2004**, *4*, 587–590.
- (3) Wang, Z. L. *J. Phys.: Condens. Matter* **2004**, *16*, R829–R858.
- (4) Wang, X.; Zhou, J.; Song, J.; Liu, J.; Xu, N.; Wang, Z. L. *Nano Lett.* **2006**, *6*, 2768–2772.
- (5) Arnold, M. S.; Avouris, Ph.; Pan, Z. W.; Wang, Z. L. *J. Phys. Chem. B* **2003**, *107*, 659–663.
- (6) Lee, C. J.; Lee, T. J.; Lyu, S. C.; Zhang, Y.; Ruh, H.; Lee, H. J. *Appl. Phys. Lett.* **2002**, *81*, 3648–3650.
- (7) Hughes, W. L.; Wang, Z. L. *Appl. Phys. Lett.* **2003**, *82*, 2886–2888.
- (8) Palaci, I.; Fedrigo, S.; Brune, H.; Klinke, C.; Chen, M.; Riedo, E. *Phys. Rev. Lett.* **2005**, *94*, 175502.
- (9) Nam, C.-Y.; Jaroenapibal, P.; Tham, D.; Luzzi, D. E.; Evoy, S.; Fischer, J. E. *Nano Lett.* **2006**, *6*, 153–158.
- (10) Chen, C. Q.; Shi, Y.; Zhang, Y. S.; Zhu, J.; Yan, Y. J. *Phys. Rev. Lett.* **2006**, *96*, 075505.
- (11) Liu, K. H.; Wang, W. L.; Xu, Z.; Liao, L.; Bai, X. D.; Wang, E. G. *Appl. Phys. Lett.* **2006**, *89*, 221908.
- (12) Li, X.; Wang, X.; Xiong, Q.; Eklund, P. C. *Nano Lett.* **2005**, *5*, 1982–1986.
- (13) Bai, X. D.; Gao, P. X.; Wang, Z. L.; Wang, E. G. *Appl. Phys. Lett.* **2003**, *82*, 4806–4808.
- (14) Yum, K.; Wang, Z.; Suryavanshi, A. P.; Yu, M.-F. *J. Appl. Phys.* **2004**, *96*, 3933–3938.
- (15) Ni, H.; Li, X. *Nanotechnology* **2006**, *17*, 3591–3597.
- (16) Mai, W.; Wang, Z. L. *Appl. Phys. Lett.* **2006**, *89*, 073112.
- (17) Kulkarni, A. J.; Zhou, M.; Ke, F. J. *Nanotechnology* **2005**, *16*, 2749–2756.
- (18) Özgür, Ü.; Alivov, Ya. I.; Liu, C.; Teke, A.; Reshchikov, M. A.; Doğan, S.; Avrutin, V.; Cho, S.-J.; Morkoç, H. *J. Appl. Phys.* **2005**, *98*, 041301.
- (19) Carpick, R. W.; Ogletree, D. F.; Salmeron, M. *Appl. Phys. Lett.* **1997**, *70*, 1548–1550.
- (20) Sader, J. E.; Chon, J. W. M.; Mulvaney, P. *Rev. Sci. Instrum.* **1999**, *70*, 3967–3969.
- (21) Pan, Z. W.; Dai, Z. R.; Wang, Z. L. *Science* **2001**, *291*, 1947–1949.
- (22) Bates, C. H.; White, W. B.; Roy, R. *Science* **1962**, *137*, 993.
- (23) Saïta, A. M.; Decremps, F. *Phys. Rev. B* **2004**, *70*, 035214.
- (24) Limpijumngong, S.; Jungthawan, S. *Phys. Rev. B* **2004**, *70*, 054104.
- (25) Kulkarni, A. J.; Zhou, M.; Sarasamak, K.; Limpijumngong, S. *Phys. Rev. Lett.* **2006**, *97*, 105502.
- (26) Barnard, A. S.; Xiao, Y.; Cai, Z. *Chem. Phys. Lett.* **2006**, *419*, 313–316.
- (27) Zhang, J.-M.; Zhang, Y.; Ji, V. *Solid State Commun.* **2006**, *139*, 87–91.
- (28) Coleman, V. A.; Bradby, J. E.; Jagadish, C.; Munroe, P.; Heo, Y. W.; Pearton, S. J.; Norton, D. P.; Inoue, M.; Yano, M. *Appl. Phys. Lett.* **2005**, *86*, 203105.

NL070310G